LAUTECH Journal of Engineering and Technology 19 (5) 2025: 152-162
10.36108/laujet/5202.91.0521

Development and Performance Evaluation of a Fixed Bed pyrolyser for Valorization of Selected Biomass

Areghan, S. E., Hassan-Ajao, O. Q., *Alao, L. O. and Omoniyi, T. O.

Article Info

Article history:

Received: Sept. 11, 2025
Revised: Oct. 26, 2025
Accepted: Nov. 16, 2025

Keywords:

Machine Design, *Cola nitida* Sawdust, Biomass Volatilisation

Corresponding Author:
allukmon1@gmail.com

ABSTRACT

Efficient waste management in the forestry and wood industries is essential for conserving resources, energy, and costs. This study presents the design and fabrication of a fixed-bed pyrolysis system for the production of bio-oil, bio-char, and syngas from Cola nitida sawdust residues. The system comprises a reactor, condenser, heating unit, and discharge unit, all designed in accordance with ASTM standards (ASTM A36, ASTM C182 and ASTM C133) and fabricated at the Technical Support Unit, Faculty of Technology, University of Ibadan. Dried and sieved sawdust fractions of 0.5, 1.5, and 3.0 mm particle size and mass of 200 ±5 g mass were pyrolyzed at residence time of 30, 45 and 60 minutes respectively with three replicates runs each under controlled conditions to assess the effects of particle size and residence time on product yield and composition. Results showed that smaller particles (0.5 mm) yielded the highest liquid fraction (45.8%) due to enhanced heat transfer and rapid devolatilization, while larger sizes (1.5 - 3.0 mm) produced less bio-oil but more bio-char, with 3.0 mm yielding the most bio-char (38.7%) and prolonged residence times promoted secondary cracking, reducing liquid yield. The developed system, with a total fabrication cost of USD 173 (₦276,600), effectively volatilized Cola nitida sawdust.

INTRODUCTION

Bio-oil is a liquid product derived from the thermochemical conversion of biomass, primarily obtained through pyrolysis. Bio-oil can be produced from diverse biomass sources such as wood and wood waste, agricultural residues, animal waste, Biomass slash, and even algae (Machado *et al.*, 2022) The organic compounds identified in bio-oil with functional groups such as phenols and carboxylic acids makes it a viable raw material for chemical industries. Compared to fossil fuels, the production and utilization of bio-oil lead to lower greenhouse gas emissions and a reduced net carbon dioxide output, highlighting its potential as an environmentally friendly alternative to fossil-derived synthetic chemicals. Bio-oil has quite a number of applications but it is primarily used as fuel in boilers in the industry as an environmentally friendly substitute for the more popular fossil fuel used in the generation of energy and for heating application. Other uses for bio-oil are gaining traction and study in this field has intensified in recent years, particularly in its application as a preservative. . Mashuni *et al.* (2017) found that "the chemical components in lignocelluloses biomass bio-oil from the cocoa shell pyrolysis were ammonia, hexane, alcohol, ketone, acid and phenolic compounds which can be used as a material of preservative and pesticide applications". Bio-oil has a potential as a substitute for synthetic preservatives for treating lignocellulosic materials like wood and bamboo which are important sustainable engineering materials.

Pyrolysis is a thermochemical process that decomposes organic materials, such as biomass, in the absence of oxygen to produce bio-oil, bio-char and gaseous products. This technology has garnered significant attention as an efficient method of renewable energy production and waste management. Compared to fossil fuels, biomass-based pyrolysis contributes less to Green House Gases (GHGs) emissions, making it an

environmentally friendly solution for various applications (Pitoyo et al., 2022; Rasaq et al., 2021). The importance of pyrolysis lies in its ability to utilize diverse feed-stocks, including agricultural residue, animal waste, wood and wood waste, municipal solid waste (MSW). These feed-stocks, often considered waste, are rich in carbon and hydrogen, making them excellent raw materials for bio-oil production. The wood conversion industry generates an enormous amount of waste. Senescent *Cola nitida* wood is one of most harvested and converted species into sawn timber for various utilisation. Thus, wastes like barks, sawdust and offcuts from conversion of felled woods (*Cola nitida*) to lumbers are often a menace in the conversion yard, while the wastes are not put to good use. The waste from the debarked *Cola nitida* tree in particular is a potential feedstock for pyrolysis to produce bio-oil which can be adapted as preservatives for lignocellulosic materials like wood and bamboo. This study aimed to develop a fixed bed pyrolysis system from local materials and evaluate its performance on biomass conversion and product yield distribution.

METHODOLOGY

The system's key components such as the frame, inlet and outlet chambers, reaction chamber, and heat source were engineered based on the feedstock's properties. The design prioritized several critical factors for performance, including peak pyrolysis temperature, heating rate, vapor residence time, efficient condensation, and temperature management to guarantee safe operation and optimal output.

Reaction chamber

The reaction chamber consists of a spherical base connected to a cylindrical section. The total length of the chamber is 165 mm. The cylindrical part begins 65 mm above the base of the sphere, and the chamber has an overall diameter of 204 mm.

Volume of the reaction chamber is the sum of a and b

a. The portion of the sphere up to 65 mm height (a spherical cap) and
b. The cylindrical section above it.

i. Volume of the spherical cap (V_{cap})

The volume of a spherical cap of height *h* and radius *r* was determined from equation 1

$$V_{cap} = \frac{\pi h^2(3r-h)}{3} \quad (1)$$

Where, diameter of the chamber = 204 mm, with the radius (r) = 102 mm, h = 65 mm

$$V_{cap} = \frac{\pi(65)^2(3\times 102-65)}{3}$$
$$= \frac{\pi(65)^2(3\times 102-65)}{3}$$
$$\approx 1{,}067{,}425\, mm^3$$

ii. Volume of the cylinder ($V_{cylinder}$)

The volume of a cylinder was determined from equation 2

$$V_{cylinder} = \pi r^2 h \quad (2)$$

Where, $h = 165 - 65\, mm = 100\, mm$

$V_{cylinder} = \pi r^2 h = \pi(102\, mm)^2(100\, mm) \approx 3.269 \times 10^6\, mm^3$

iii. Total volume was determined from the summation of volume of the spherical cap and volume of cylinder

$$V_{chamber} = V_{cap} + V_{cylinder}$$
$$V_{chamber} = 1.067 \times 10^6\, mm^3 + 3.269 \times 10^6\, mm^3$$
$$= 4.336 \times 10^6\, mm^3$$

The volume of the reactor was determined in liters

$$V_{chamber} = 4{,}336{,}097\, mm^3 \times \left(\frac{1\, L}{10^6\, mm^3}\right)$$
$$= 4.336\, L$$

Estimation of maximum mass of *Cola nitida* sawdust

The density of C*ola nitida* sawdust at 12% moisture content has a density range of 0.51 – 0.57 kg/L. The mass was determined using equation 3

$$m = \rho \times V_{\{chamber\}} \quad (3)$$

Where, m =mass , ρ = density, V= volume

$$m = 0.51\frac{kg}{L} \times 4.336L = 2.211\ kg$$

The pyrolyser is designed to pyrolyse approximately 2.2 kg of C*ola nitida* sawdust

Determination of the annular thickness of the reactor

The outer diameter of the reactor is 301 mm, and the reaction chamber has a diameter of 204 mm. The insulation thickness was determined from equation 4

$$t_{insulation} = \frac{D_{outer} - D_{chamber}}{2} \quad (4)$$

$$t_{insulation} = \frac{301 - 204}{2} = 48.5\ mm$$

Thickness for insulation is 48.5 mm

Component design

The frame was intended to be designed as a tripod support developed from a 3mm thick iron angle bar of dimension 40 × 40- and 310-mm length. The three legs are evenly spaced at 120° apart to ensure stability. The tripod (as shown in Plate 1) structure provides stability while ensuring equal load distribution.

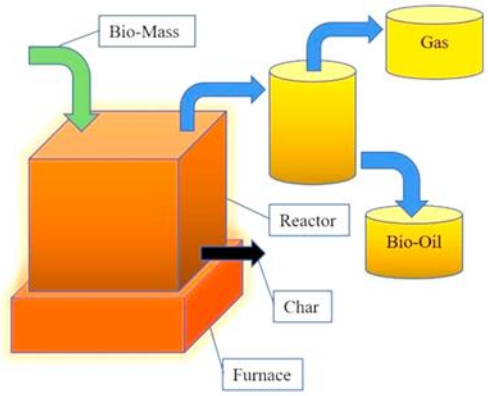

Figure 1: Sketch of a fixed-bed reactor structure (Sakthivel et al., 2023)

The estimation of the self-weight of the fixed-bed reactor is essential to the design process, as it directly affects the reactor's mechanical stability, load distribution, and support requirements. The reactor assembly comprises a mild steel cylindrical body, a fired clay ring serving as thermal insulation, and a fired clay lid used for top closure. The calculations were performed based on standard engineering density values and the geometric parameters of each component, while gravitational acceleration was assumed as 9.81 m/s². The material properties used for the analysis include a mild steel density of 7850 kg/m³ and a fired clay density of 1900 kg/m³. The cylindrical reactor has an internal volume of 4.336 litres, equivalent to 4.336×10^{-3} m³. The clay ring insulator has a thickness of 48.5 mm (0.0485 m), a height of 100 mm (0.1 m), and an inner radius of 100 mm (0.1 m). The clay lid possesses a diameter of 204 mm (0.204 m) and a thickness of 48.5 mm (0.0485 m). These parameters formed the basis for the derivation of mass and weight for each reactor component.The mass of the mild steel section was determined using the general relation between mass, density, and volume, expressed as M = ρV (Richards, 2021).

Substituting the given parameters, the mass of the steel component was obtained as: Ms = 7850 × 4.336×10^{-3} = 34.04 kg. The corresponding weight was then evaluated using the specific weight relation W = mg (Meriam & Kraige, 2018), giving: Ws = 34.04 × 9.81 = 334.67 N. Hence, the self-weight of the steel body was approximately 334.67 N. The fired clay ring, modelled as a hollow cylinder, had its volume determined from the geometric relation Vr = πh[(ri + tr)² − ri²] (Mott *et al.*, 2023). Substituting the respective values yields: Vr = π(0.1)[(0.1 + 0.0485)² − 0.1²] = 0.003321 m³. With the density of fired clay taken as ρr = 1900 kg/m³ (Ashby & Jones, 2022), the mass and weight were computed as:

Mr = 1900 × 0.003321 = 6.31 kg

Wr = 6.31 × 9.81 = 61.91 N

For the clay lid, idealized as a solid circular disc, the radius was derived as rl = Dl / 2 = 0.102 m. The volume was calculated using the standard expression V = πr²t (Meriam & Kraige, 2018): Vl =

$\pi(0.102)^2(0.0485) = 0.001587$ m³. The corresponding mass and weight were obtained as:

Ml = 1900 × 0.001587 = 3.02 kg

Wl = 3.02 × 9.81 = 29.58 N

Summing up the contributions of all components, the total mass and total weight of the reactor assembly were determined as:

Mtotal = 34.04 + 6.31 + 3.02 = 43.37 kg

Wtotal = 43.37 × 9.81 = 425.46 N

Thus, the combined self-weight of the reactor system is approximately 425 N .The load estimated to be distributed evenly across the tripods is 425N, equation 5 is used for the determination of the load on each tripod

$$F_{leg} = W/3 \quad (5)$$

Load distribution of the pyrolyser frame was determined $F_{leg} = 425/3 = 141.67N \approx 0.142$KN

The critical buckling load for a column was determined using Euler's formula, as presented in equation 6

$$P_{cr} = \frac{\pi^2 EI}{(KL)^2} \quad (6)$$

Where: I = Moment of Inertia of angle bar, K = Effective length factor. Thus, (K) for fixed-pinned: 0.7, L = Length = (310 mm = 0.31 m) E = Modulus of elasticity of the material

To determine the Moment of Inertia (*I*) for an L-section angle bar, equation 7 was used

$$I = 1/12(b_2h_2^3 - b_1h_1^3) \quad (7)$$

Where, I = Moment of Inertia of angle bar, b=width, h =height, ($_1$ and $_2$ represent the two rectangles that form the L shape)

$$I = 1.85 \times 10^{-8}\, m^4$$

Substituting values, I equation 2 and 3 into equation 1 (Euler's formula)

$$P_{cr} = \frac{\pi^2(200\times10^9)(1.85\times10^{-8})}{(0.7\times0.31)^2} = 24{,}200\, N$$

Since $P_{cr} = 24{,}200\, N$ is much greater than 141.67 N per leg, the tripod legs are Structurally safe from buckling

Condenser Frame

The Condenser is supported on four legs which serve as the base for the condensing vessel as shown in Plate 1. The base is constructed using iron angle bars of 40 mm × 40 mm × 3 mm thickness and a length of 480 mm. The four-leg support is constructed by welding.

Estimation of the Total Load of a Mild Steel Cylindrical Shell Condenser

The geometric and physical properties of the cylindrical shell condenser were utilized to estimate its total self-weight, including the mass contribution of the contained water. The parameters used in the analysis are as follows: diameter of cylinder (D) = 0.320 m, height of cylinder (h) = 0.355 m, density of mild steel (ρs) = 7850 kg/m³, density of water (ρw) = 1000 kg/m³, and gravitational acceleration (g) = 9.81 m/s². The volume of the condenser shell was determined using the standard geometric relation for a right circular cylinder, expressed as $V = \pi r^2 h$ (Mott *et al.*, 2023), where the internal radius (r) is given by r = D/2 = 0.320/2 = 0.160 m. Substituting these parameters gives:

$V = \pi(0.160)^2(0.355) = 3.1416 \times 0.0256 \times 0.355 = 0.02853$ m³.

Hence, the internal volume of the cylindrical condenser shell is 0.02853 m³. The mass of the mild steel shell was evaluated using the general mass–density relation $m = \rho V$ (Richards, 2021). Substituting the known values:

Ms = $\rho s \times V = 7850 \times 0.02853 = 224.36$ kg. When filled with water, the water mass was similarly obtained from $M = \rho V$, taking the density of water as $\rho w = 1000$ kg/m³ (Meriam & Kraige, 2018): Mw = 1000 × 0.02853 = 28.53 kg. The total combined mass of the condenser and the water content was therefore determined as:

Mtotal = Ms + Mw = 224.36 + 28.53 = 252.89 kg.

To obtain the total load exerted by the condenser system, the weight was evaluated using the standard gravitational relation W = mg (Hibbeler, 2022):

Wtotal = 252.89 × 9.81 = 2479.84 N.

Thus, the total weight of the condenser assembly, including the contained water, is approximately 2479.8 N (≈ 2.48 kN). Equation 8 was used to determine the estimated load distributed evenly by each of the four legs,

$$F_{leg} = \frac{W}{4} \quad (8)$$

$$F_{leg} = \frac{W}{4} = \frac{2479.8}{4} = 619.95\ N$$

Where, F_{leg} = force on each leg , w = weight of the condenser

The L-section angled iron bars have the same cross section as that used for the construction of the base of the pyrolyser. Moment of inertia determined was $= 1.85 \times 10^{-8}\ m^4$.

Using equation 2(Euler's Formula) to determine the buckling

$$P_{cr} = \frac{\pi^2(200\times10^9)(1.85\times10^{-8})}{(0.7\times0.48)^2} = 9,360\ N$$

Since $P_{cr} = 9{,}360$ N is much greater than 619.95 N, the four-leg support is structurally safe

Burner (heat source)

Heat energy required for pyrolysis was estimated using the equation 9

$$Q = mc_p\Delta T \quad (9)$$

Where, $m = 2.17\ kg$ (Mass of Cola nitida sawdust), $C_p = 1.76\frac{kJ}{kg}\cdot K$ (Specific heat capacity of biomass), $\Delta T = 500\ K$ (Assumed temperature rise)

$$Q = 2.17\ kg\ x\ 1.76\frac{kJ}{kg}\cdot K\ x\ 500\ K$$

$$= 1907.3\ KJ$$

he Burner must be able to generate 1.91 MJ of energy

Condenser design

Heat transfer in the condenser

To efficiently condense pyrolysis vapor, the heat dissipation rate needed to be determined. Equation 10 can be used to determine the heat dissipation rate using the heat transfer equation.

$$Q = m_{vapor}c_p\,\Delta T \quad (10)$$

Where, Q = Heat to be removed (J), m_{vapor} = 0.651kg, Mass of pyrolysis vapors assumed equal to 30% of maximum biomass mass, 2.17 kg ranging from 20% to 40% (Jerzak *et al*, 2024), c_p = 2.0 kJ/kg·K, Specific heat of pyrolysis (Yang et al., 2021), ΔT = Cooling from 400°C to 40°C = 360 K

$$Q = (2.17)(2.0)(360) = 1561.2\ kJ$$

1.56 MJ of heat is transferred from the condenser

Cooling Water Flow Rate determination

The heat absorbed by water was determined from equation 11

$$Q = m_{water}\ x\ C_{pwater}\ x\ \Delta T \quad (11)$$

Where, C_{pwater} = 4.18 kJ/kg·K. Specific heat capacity of water, ΔT = Assumed 15K (from 25°C to 40°C)

Rearranging for mass flow rate of water

$$m_{water} = \frac{Q}{C_{pwater} * \Delta T} = \frac{1561.2KJ}{4.18\ kJ/kg\cdot K * 15K} = 24.9\ kg = 24.9\ L/min$$

Thus, the condenser must have a cooling water flow rate of approximately 25 L/min

Discharge Unit

The design of the pyrolytic oil collection system facilitates the natural drainage of condensed liquids, preventing accumulation and potential blockages. Standard engineering practices suggest that an inclination angle of at least 1°–2% (Ashrae, 2021; International Code Council (ICC), 2021) is sufficient for liquid flow in drainage pipes. In pyrolysis systems, steeper inclines up to 5° may be employed to handle viscous pyrolytic oils (Zhou et al., 2022)

Fabrication Process

The fabrication was done in the Welding Unit of the Technical Support Unit (TSU), faculty of technology, University of Ibadan, Ibadan, Nigeria using locally sourced materials. Parts were first measured using a measuring tape, as shown in Plate 1a. They were then cut into the necessary sizes using a grinding machine, and on occasion, a hacksaw with a blade, as shown in Plate 1b. The arrangement

and welding of the angle iron is depicted in Plate 1c. The angle iron metal measuring 40 x 40 mm was tackled to start the tripod frame welding process. As presented in Plate 1d, it was welded at a straight angle to one another to provide rigidity and facilitate the simple attachment of the frame top. As seen in Plate le, the top of the frame was made of iron sheet metal with a 4 mm gauge. After that, the top member was positioned and welded to the frame in the manner depicted in Plate 1f.

Cost of Fabrication

The pyrolyser machine was estimated to have cost N276,600:00 ($173) to fabricate, based on a rate of N1600 to $1, as Table 2, presents the bill of materials.

Table 1: Part and Material of Construction and Quantity Specification

s/n	Component	Material	Specifications	Dimension (mm)	Reason for selection
1	Tripod legs frame	Mild Steel	L-section 40 × 40 angle iron bar	3x (40×40) ×310	Durability and affordability
2	Condenser frame	Mild Steel	L-section 40 × 40 angle iron bar	3x (40×40) ×480	Durability and affordability
3	Reaction chamber	Metal plate	spherical base and cylinder	65x165x204	Durability and affordability
4	Annular space	Clay	Circular	48.5	Heat absorption and retaining
5	Burner	Gas		1.91 M J	Efficient energy rating

(a) (b) (c) (d)

Plate 1(a-d): (a) Reactor mounted on three angled iron bar (b) Reaction chamber and the top flange (c) Reactor lid with rectangular flange (d) Reactor and lid with flange on both

(e) (f) (g) (h)

Plate 1(e-h): (e) Wire mesh welded to the lid (f) Reactor lid with pipe as vent (g) Lining the reactor with refractory clay (h) Reactor lined with refractory clay

Plate 1(i-j) (i): Condenser mounted on iron angle bar (j): Shell-type water-cooled condenser system (k): Reactor system with burner (l): The Fixed bed pyrolyser

Plate 1(a-l): Construction Process of the Fixed Bed Pyrolyser

Table 2: Bill of Engineering Material and Estimate for the Machine

Item	Specification	Quantity	Unit Price (N)	Total (N)
Reactor	Mild steel drum	2	20000	40,000
Angle bar	5 mm thickness	2	15,000	30,000
Insulation	Clay reflective lining	1	30,000	30,000
Condenser	Vessel	1	20,000	20,000
Connecting Pipe	Stainless steel, 1-inch diameter	1	10,000	10,000
Gas Burner	200mm diameter	1	20,000	20,000
Thermocouple	For temperature monitoring	1	5,000	5,000
Control Unit	Switch, temperature controller, cable, and plug	1	35,000	35,000
Workmanship		1	40,000	40,000
Transportation		-	20,000	20,000
Gas Refill		-	10,000	10,000
Gas Tube		3 yards	700	2100
Gas Control		1	4,500	4,500
Miscellaneous		-	10,000	10,000
Total				**276, 600**

Collection, preparation and processing of biomass feedstock

The biomass used for pyrolysis in this study was *Cola nitida* sawdust. It was immediately collected after conversion of *Cola nitida* wood in a wood conversion shop in Bodija Plank Market Ibadan, Oyo State, Nigeria. Approximately 5 kg of *Cola nitida* sawdust was gathered from milling operations, which typically generate fine particulate wood waste as a by-product. Then, the biomass (*Cola nitida* sawdust at moisture content of 30%) was subjected to air drying in a well-ventilated area for five days to bring the moisture content to 12% (Plate 2). Prior to drying, the sawdust was sieved into three distinct particle size ranges of 0.5, 1.5 and 3 mm using ASTM E11 standard test sieves. The

sieved materials were then stored in airtight plastic containers under ambient laboratory conditions (25–28 °C) to maintain their dryness and prevent contamination prior to pyrolysis experiments.

Plate 2: Air Drying of the *Cola nitida* Sawdust

Pyrolysis of *Cola nitida* Sawdust

The reactor provided heat, and pressure required in the absence of oxygen for the valorisation of the *Cola nitida* sawdust samples. The pyrolyser (machine) capacity and the pyrolysis efficiency was determined for *Cola nitida* sawdust samples of 200 ±5 g from particle sizes (0.5, 1.5, and 3.0 mm) at moisture content below 12%, respectively. Processing or pyrolysis time for each sample of particle sizes (0.5, 1.5, and 3.0 mm) were done at temperatures ranging from 300ºC -500ºC with residence time of 30, 45, and 60 mins respectively. Three replicates were pyrolysed from each of the particle sizes.

Performance Evaluation

The performance evaluation of a fixed bed pyrolyser is predominantly assessed through the yield distribution of its three main products: bio-oil (liquid), bio-char (solid), and syngas (bio-gas). These product yields serve as direct indicators of the efficiency and suitability of the reactor for biomass conversion under specific process conditions. Understanding the yield distribution helps optimize design parameters and operational settings for targeted product maximisation, particularly in thermochemical valorisation of biomass like *Cola nitida* sawdust. The yields are estimated considering operational factors like particle size and residence time.

i. Bio-char yield

Bio-char is the solid carbonaceous residue obtained post-pyrolysis, typically representing the fixed carbon and ash content retained in the biomass. The bio-char yield is influenced by feedstock properties (e.g., particle size, moisture content), pyrolysis temperature, and heating rate.

$$Biochar\ Yield\ (\%) = \left(\frac{Mass\ of\ biochar\ collected}{Mass\ of\ dry\ feedstock}\right) \times 100 \quad (11)$$ (Awad *et al.*, 2024)

i. Bio-oil yield

Bio-oil is the liquid fraction containing a complex mixture of oxygenated hydrocarbons. It is the most economically desirable product in pyrolysis aimed at renewable fuel applications.

$$Bio-oil\ Yield\ (\%) = \left(\frac{Mass\ of\ bio-oil\ collected}{Mass\ of\ dry\ feedstock}\right) \times 100 \quad \ldots (12)$$

(Awad *et al.*, 2024)

i. Syngas Yield

Syngas comprises non-condensable gases including CO, CO_2, H_2, and CH_4. Its yield increases at higher pyrolysis temperatures and with lower biomass moisture content. While not directly collected in the present design, the performance of the reactor in terms of syngas yield was inferred from mass balance calculations.

$$Gas\ Yield\ (\%) = \left(\frac{Mass\ of\ gas\ collected}{Mass\ of\ dry\ feedstock}\right) \times 100 \quad (13)$$

Alternatively,

$$Gas\ Yield\ (\%) = 100 - ((Bio-oil\ Yield\ (\%)) + (Biochar\ Yield\ (\%)) \quad (14)$$

(Jerzak *et al.*, 2024; Igliński *et al.*, 2023)

Results

Pyrolysis Yield by Particle Size

The distribution of pyrolytic products across three particle sizes (0.5, 1.5, and 3.0 mm) as presented in

Figure 2. The yield values recorded for bio-oil, bio-char and bio-gas from 0.5 mm particle size, were 49.0%, 30.8%, and 24.2%; however, from 1.5 mm particle size, the corresponding values were 42.5%, 34.0%, and 23.5%, while from 3.0 mm particle size, the values obtained were 37.5%, 38.0%, and 24.5%, respectively.

Effect of Particle size

The study found that particle size significantly influences product distribution in pyrolysis. The 0.5 mm particle class yielded the highest liquid fraction, while larger particles decreased liquid yield. Bio-char production increased from 30-31% at 0.5 mm to 34-35 wt% at 1.5 mm and 38 wt% at 3.0 mm. Non-condensable gases yielded 24-25 wt%. Smaller particles promote uniform heating and rapid de-volatilization, while larger particles retain hot volatiles, affecting liquid yield. . Maintaining feedstock particle size below 1 mm is a high-leverage strategy.

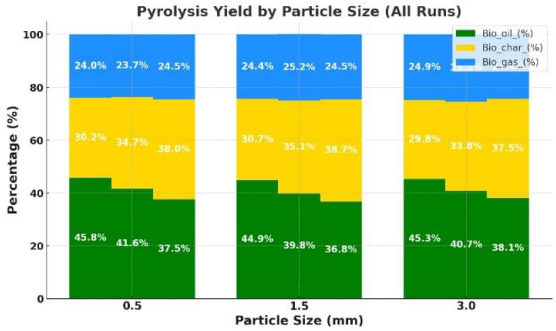

Figure 2: Pyrolysis Yield for by Particle Size for all the Samples Run as Aggregate Percent of the Pyrolysis Product

Normalised Yield by Residence Time

The normalised yield distribution of pyrolytic products at residence times of 30, 45, and 60 minutes for particle size 0.5 mm, 1.5 mm and 3.0 mm respectively is presented in Figure 3. At 30 minutes, the normalised values were 45.2%, 30.5%, and 24.3%; at 45 minutes, the respective yields were 41.0%, 34.5%, and 24.5%; and at 60 minutes, the corresponding values were 38.0%, 38.0%, and 24.0%, for bio-oil, bio-char and bio-gas respectively.

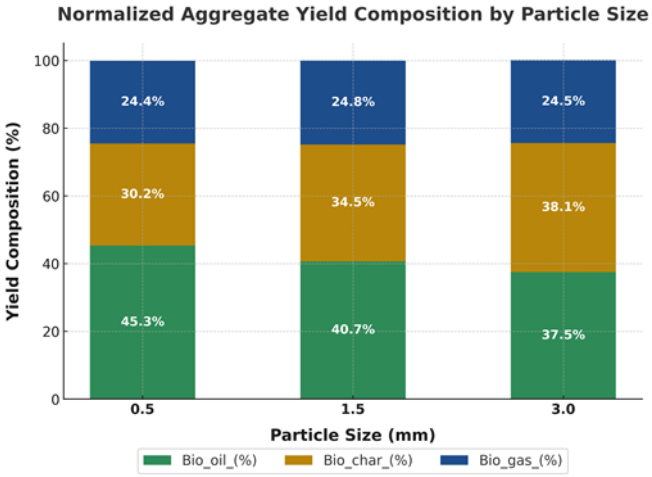

Figure 3: Normalised Aggregate Yield of Pyrolysis Products by Percentage According to Residence Time of Each Particles Size Class

Effect by Residence Time

The study observed an inverse relationship between liquid and char fractions in fixed-bed pyrolysis systems. The liquid (bio-oil) yield decreased from 45% at 30 minutes to 41% at 45 minutes and 38% at 60 minutes, while the bio-char yield increased. Longer residence times facilitate secondary cracking and condensation reactions, such as coking, which reduce the liquid fraction. This highlights the long vapour residence time in fixed-bed pyrolysis systems.

Conclusion

The design and fabrication of the fixed-bed pyrolysis system using locally available materials demonstrated an effective, low-cost, and sustainable approach to biomass conversion for renewable energy production. The system successfully converted selected biomass, *Cola nitida* sawdust, into valuable bio-products (bio-oil, bio-char, and syngas) through controlled thermal decomposition. Experimental results revealed that particle size and residence time significantly influenced product yield distribution and quality. Specifically, finer particles (0.5 mm) exhibited superior heat transfer efficiency and rapid devolatilization, resulting in the

highest bio-oil yield of 45.8%, while coarser fractions (1.5–3.0 mm) favored bio-char formation, with 3.0 mm producing the highest char yield of 38.7%. Extended residence time encouraged secondary cracking reactions, thereby reducing liquid yield and enriching gaseous products.

Economically, the total fabrication cost of USD 173 (₦276,600) underscores the system's affordability and potential scalability for small and medium-scale biomass valorization. Technically, the reactor's performance confirmed stable operation and efficient thermal conversion, validating the design parameters and material selection. Environmentally, this work supports sustainable waste management within the forestry and wood industries by transforming sawdust residues into energy-rich products, contributing to cleaner production and circular economy objectives.

Overall, the study established that a locally fabricated fixed-bed pyrolysis system can reliably achieve efficient biomass conversion and yield optimization. Future research should focus on product upgrading, emission profiling, and continuous-feed design optimization to enhance system efficiency and broaden industrial applicability in renewable energy generation.

REFERENCES

Anokye, R., Boadu, K. B., Fianko, C. N., and Amegashiti, V. B. (2024). The chemical composition of Savannah bamboo (Oxytenanthera abyssinica) vinegar at varying pyrolysis temperatures and its termiticidal activity against wood-feeding termites. Advances in Bamboo Science, 6, 100063. https://doi.org/10.1016/j.bamboo.2024.100063

Ashby, M. F., & Jones, D. R. H. (2022). *Engineering Materials 1: An Introduction to Properties, Applications and Design* (5th ed.). Elsevier. https://doi.org/10.1016/C2020-0-00724-1

Ashrae. (2021). Ashrae Handbook Fundamentals. American Society of Heating, Refrigerating and Air-Conditioning Engineers.

Awad, M. I., Makkawi, Y., & Hassan, N. M. (2024). Yield and Energy Modeling for Biochar and Bio-Oil Using Pyrolysis Temperature and Biomass Constituents. ACS omega, 9(16), 18654–18667. https://doi.org/10.1021/acsomega.4c01646

Hibbeler, R. C. (2022). *Engineering Mechanics: Statics and Dynamics* (15th ed.). Pearson Education.

Khurmi R. S. and J. K. Gupta 2005 A textbook for the Student of B.E/B.Tech. *U.P.S.C (Engg. services) Section 'B' of A.M.I.E* 1:2. 665

Igliński, B., Kujawski, W., & Kiełkowska, U. (2023). Pyrolysis of waste biomass: technical and process achievements, and future development—a review. Energies, 16(4), 1829.

International Code Council (ICC). (2021). International Plumbing Code. ICC.

Isukuru, E. J., Ogunkeyede, A. O., Adebayo, A. A., and Uruejoma, M. F. (2023). Potentials of Bamboo and its Ecological Benefits in Nigeria. Advances in Bamboo Science, 4, 100032.

Jerzak, W., Acha, E., & Li, B. (2024). Comprehensive review of biomass pyrolysis: Conventional and advanced technologies, reactor designs, product compositions and yields, and techno-economic analysis. Energies, 17(20), 5082.

Kumar, R., Strezov, V., Weldekidan, H., He, J., Singh, S., Kan, T., and Dastjerdi, B. (2020). Lignocellulose biomass pyrolysis for bio-oil production: A review of biomass pre-treatment methods for production of drop-in fuels. Renewable and Sustainable Energy Reviews, 123, 109763. https://doi.org/10.1016/j.rser.2020.109763

Machado, H., Cristino, A. F., Orišková, S., & Galhano dos Santos, R. (2022). Bio-oil: the next-generation source of chemicals. Reactions, 3(1), 118-137.

Meriam, J. L., & Kraige, L. G. (2018). *Engineering Mechanics: Dynamics* (7th ed.). Wiley.

Mashuni, Jahiding, M., Kurniasih, I., and Zulkaidah. (2017). Characterization of preservative and pesticide as potential of bio oil compound from pyrolysis of cocoa shell using gas chromatography. 020008. https://doi.org/10.1063/1.4978081

Mott, R. L., Vavrek, E. M., & Wang, J. (2023). *Applied Strength of Materials* (7th ed.). CRC Press. https://doi.org/10.1201/9781003198604

Pavate, V., Jagdale, A., Shinde, R., Manechikkannara, N., and Patil, D. (2024). Study on Bamboo Industry. International Journal for Research in Applied Science and Engineering Technology, 12(4), 1533–1548. https://doi.org/10.22214/ijraset.2024.60085

Pitoyo, J., Suharto, T. E., and Jamilatun, S. (2022). Bio-oil from Oil Palm Shell Pyrolysis as Renewable Energy: A Review. CHEMICA: Jurnal Teknik Kimia, 9(2), 67. https://doi.org/10.26555/chemica.v9i2.22355

Richards, D. (2021). *Basic Engineering Science: A Systems Accounting and Modeling Approach*. LibreTexts Engineering. https://eng.libretexts.org

Rasaq, W. A., Golonka, M., Scholz, M., and Białowiec, A. (2021). Opportunities and Challenges of High-Pressure Fast Pyrolysis of Biomass: A Review. Energies, 14(17), 5426. https://doi.org/10.3390/en14175426

Sakthivel, R., Harshini, G. V., Vardhan, M. S., Vinod, A., and Gomathi, K. (2023). 3—Biomass energy conversion through pyrolysis: A ray of hope for the current energy crisis. In V. K. Singh, N. Bangari, R. Tiwari, V. Dubey, A. K. Bhoi, and T. S. Babu (Eds.), Green Energy Systems (pp. 37–68). Academic Press. https://doi.org/10.1016/B978-0-323-95108-1.00006-9

Zhou, M., Li, X., and Wang, Y. (2022). Design optimization of pyrolysis condensate collection systems. Renewable Energy, 192, 412–420. https://doi.org/10.1016/j.renene.2022.04.045